

Published in final edited form as:

*J Phys Chem Lett.* 2019 April 18; 10(8): 1900–1907. doi:10.1021/acs.jpcclett.9b00555.

## Quantum Roaming in the Complex Forming Mechanism of the Reactions of OH with formaldehyde and methanol at Low Temperature and Zero Pressure: A Ring Polymer Molecular Dynamics Approach

Pablo del Mazo-Sevillano<sup>†</sup>, Alfredo Aguado<sup>†</sup>, Elena Jiménez<sup>‡,||</sup>, Yury V. Suleimanov<sup>¶,⊥</sup>, and Octavio Roncero<sup>\*,§</sup>

<sup>†</sup>Unidad Asociada UAM-CSIC, Departamento de Química Física Aplicada, Facultad de Ciencias M-14, Universidad Autónoma de Madrid, 28049, Madrid, Spain

<sup>‡</sup>Departamento de Química Física, Facultad de Ciencias y Tecnologías Químicas, Universidad de Castilla La Mancha, Avda. Camilo José Cela 1B, 13071 Ciudad Real, Spain

<sup>¶</sup>Computation-based Science and Technology Research Center, Cyprus Institute, 20 Kavafi Str., Nicosia 2121, Cyprus

<sup>§</sup>Instituto de Física Fundamental (IFF-CSIC), C.S.I.C., Serrano 123, 28006 Madrid, Spain

<sup>||</sup>Instituto de Investigación en Combustión y Contaminación Atmosférica, Universidad de Castilla La Mancha, Camino de Moledores s/n, 13071 Ciudad Real, Spain

<sup>⊥</sup>Department of Chemical Engineering, Massachusetts Institute of Technology, 77 Massachusetts Ave., Cambridge, Massachusetts 02139, United States

### Abstract

The quantum dynamics of the title reactions are studied using the Ring Polymer Molecular Dynamics (RPMD) method from 20 to 1200 K using recently proposed full dimensional potential energy surfaces which include long range dipole-dipole interactions. A V-shaped dependence of the reaction rate constants is found with a minimum at 200-300 K, in rather good agreement with the current experimental data. For temperatures above 300 K the reaction proceeds following a direct H-abstraction mechanism. However, below 100 K the reaction proceeds via organic-molecule...OH collision complexes, with very long lifetimes, longer than  $10^{-7}$  s, associated to quantum roaming arising from the inclusion of quantum effects by the use of RPMD. The long lifetimes of these complexes are comparable to the time scale of the tunnelling to form reaction products. These complexes are formed at zero pressure due to quantum effects and not only at high pressure as suggested by Transition State Theory (TST) calculations for OH + methanol and other OH reactions. The zero-pressure rate constants reproduce quite well measured ones below 200 K, and this agreement opens the question of how important the pressure effects on the reaction rate constants are, as implied in TST-like formalisms. The zero pressure mechanism is the only applicable to very low gas density environments, such as the interstellar medium, unrepeatably by the experiments.

## Keywords

Ring-polymer molecular dynamics; chemical kinetics; astrochemistry; low temperatures; quantum effects; quantum roaming

Hydroxyl radical, OH, is one of the main oxidants in the atmosphere<sup>1,2</sup> and in many combustion reactions.<sup>3</sup> It reacts with many organic molecules with strong dipole moments, such as alcohols, ethers, etc, and the reaction rate constants increase enormously below 200 K.<sup>4</sup> This increase has an enormous potential impact on astrochemistry, in which organic molecules are thought to be formed on ices<sup>5–8</sup> because at the low temperatures of interest,  $\approx 10$  K, barriers inhibit the reactions. However, the molecules formed on ices do not desorb at 10 K<sup>9,10</sup> and the question of how molecules, like formaldehyde and methanol, are detected in the gas phase in cold and dense molecular clouds is still under debate.

Using a uniform supersonic gas expansion technique (CRESU, acronym in French) Heard and co-workers<sup>11</sup> reported that the OH + CH<sub>3</sub>OH reaction accelerates by 1-2 orders of magnitude when decreasing the temperature from 200-300 K to 100 K or below. This non-Arrhenius behavior was also found by other authors<sup>12–14</sup> and in many other reactions of OH with organic compounds<sup>4,15–18</sup> all using the CRESU technique. In these experiments, a V-shaped temperature dependence for the rate constant was found, with a minimum at about 200-300 K for all of the reactions, independently of the height of the reaction barrier. In all these cases the acceleration of the reaction below 100 K is explained by the formation of collision complexes between reactants and tunneling through the reaction barrier.<sup>4</sup> However, some controversy still persists.

For OH + CH<sub>3</sub>OH, Siebrand and co-workers<sup>19</sup> found that the imaginary frequency at the saddle points used in Ref.11 was too large, and that, when using the proper one, the tunneling was too slow to reproduce the measured rate constants. As an alternative, they proposed a model based on the formation of methanol dimers during the expansion: when the dimers collide with OH they lead to the formation of the CH<sub>3</sub>OH-OH complex, below the CH<sub>3</sub>OH + OH re-dissociation limit, that can only be destroyed by tunneling towards the products. Siebrand and co-workers<sup>19</sup> also predicted that the OH-reactivity of methanol dimers had to be much higher than that of the monomer. Within this model, a high density of dimers is necessary to reproduce the experimental data. The dimer density required in the simulations, however, seems to be too high according with the experimental conditions<sup>20,21</sup> to be responsible of the observed increase in the rate constant at  $T < 200$  K.

The fast increase of the rate constant for the OH + methanol reaction with decreasing temperature can be explained by transition state theory (TST) assuming that the high pressure limit (HPL) is reached.<sup>22,23</sup> In these studies the low pressure limit for the reaction was described differently. Gao *et al.*<sup>22</sup> considered a direct H-abstraction process without any stabilized pre-reactive complex formed. On the contrary, Ocaña *et al.*<sup>23</sup> used RRKM calculations, where the complex energy is determined by the nascent energy distribution above the dissociation energy at the temperature considered.

In the HPL situation, the pre-reactive complexes are stabilised by collisions with the buffer gas (BG) (more than three orders of magnitude more abundant than any reactant) used in the experiments, probably in a sequential way: first, the organic molecules (OM) complexes with the buffer gas forming  $OM \cdots BG$ , and, second, the OH reactant, formed after the nozzle by photolysis, collides with this complex leading to the formation of the  $OM \cdots OH$  collision complex. Since the BG can take some energy, the  $OM \cdots OH$  complex has a broader energy distribution than at the zero pressure limit (ZPL), with a portion below the  $OM + OH$  redissociation limit (see Fig. 1 for the  $OH + H_2CO$  reaction). At the HPL, these complexes can live long enough to tunnel through the reaction barrier to form the products. This mechanism under HPL conditions can qualitatively explain the experimental observations and, in principle, would depend on the nature of the BG.

Recently, quasi-classical trajectory (QCT) calculations on the reactions of  $H_2CO$ <sup>17,24</sup> and  $CH_3OH$ <sup>25</sup> with OH have been studied using full dimensional potential energy surfaces (PES). These studies indicate that for low temperatures the reactions take place through the formation of collision complexes, with lifetimes of several picoseconds. For  $H_2CO + OH$  it is found that the QCT rate constants are very similar to the measured ones<sup>17,24</sup> while for  $CH_3OH + OH$  they do not increase enough at low temperature.<sup>25</sup> Below 100 K, quantum effects are expected to play an important role, namely zero-point energy (ZPE) and tunneling effects. The aim of this work is then to re-evaluate the reaction mechanism under ZPL conditions by including quantum effects in full dimension dynamical simulations focussing in the reactions of OH with formaldehyde and methanol at low temperatures.

Given the high dimensionality of the reactions under examination, rigorous quantum methods are not feasible to study the reaction dynamics, and reduced dimension approaches are also expected not to be adapted because they reduce the density of states. In addition, complex forming reactions present additional difficulties for quantum dynamics as recently reviewed.<sup>26</sup> For these reasons, in this work we apply the Ring Polymer Molecular Dynamics (RPMD) method.<sup>27–31</sup> RPMD is a semiclassical formalism based on Path Integral Molecular Dynamics (PIMD) which includes quantum effects such as ZPE<sup>32</sup> and tunneling,<sup>33</sup> and it has been demonstrated to be a very powerful technique to describe reaction dynamics for various profiles of reaction path including barriers and deep wells.<sup>31</sup> In this work, we extend these RPMD studies to the title reactions which involves roaming reaction pathways and show the importance of including quantum effects for accurate estimation of reaction rate constants at low temperatures. We use the dRPMD program,<sup>34</sup> a direct version of the RPMD method based on the RPMDrate code,<sup>35</sup> which is parallelized specifically to describe long time dynamics. This direct RPMD trajectory approach involves two steps: thermalization and real-time dynamics.

The thermalization step is essentially a constrained PIMD simulation, performed in our case using the Andersen thermostat<sup>36</sup> and keeping constant the distance between the centers of mass of the two reactants, at 120 bohr in this case. After a thermalization time of 2-5 ps, the thermostat is removed, and the system is rotated so that the relative velocity vector is set parallel to the z-axis. Furthermore, a maximum impact parameter between centroids is also set, similarly to what is done in QCT approaches, to improve the statistics. In the second step, the real time dynamics is studied, with no thermostat, until the system reacts or

becomes trapped. Some details of the convergence checks are described in the supplementary information (SI).

In the second real-time dynamics part, a system consisting of  $N_{atoms} \times N_{beads}$  is propagated using a symplectic operator with a time step of 0.1 fs, needed to reproduce the high frequency modes (with  $N_{atoms}$  being the number of atoms, and  $N_{beads}$  the number of replica or beads of each atom). At the end of each RPMD trajectory the centroids are analyzed to determine whether or not the system has reacted. The rate constant is calculated according to the expression

$$k_{\beta}(T) = p_e(T) \sqrt{\frac{8k_B T}{\pi \mu}} \times \pi [b_{max}^{\beta}(T)]^2 \times P_{\beta}(T). \quad (1)$$

The index  $\beta$  refers to either the reaction (hereafter called direct reaction rate constant,  $k_{dir}$ ) or trapping ( $k_{trap}$ ), where  $P_{\beta}(T) = N_{\beta}/N_{max}$  is the probability for channel  $\beta$ , with  $N_{max}$  being the total number of RPMD trajectories and  $N_{\beta}$  is the number of trajectories leading to products or trapped in the entrance channel until a maximum propagation time  $t_{max}$ . The parameters used in the calculations are listed in Table 1.  $b_{max}^{\beta}(T)$  is the maximum impact parameter for channel  $\beta$ , reaction or trapping, at temperature T. Finally,  $p_e(T) = 1/[1 + \exp(-200.3/T)]$  is the relative population of the ground  $^2\Pi_{3/2}$  spin-orbit states of OH( $^2\Pi$ ), which is introduced under the assumption that only the ground spin-orbit state reacts.

The direct reaction rate constants,  $k_{dir}(T)$ , in Table 1 decreases monotonously with decreasing temperature. On the contrary, the trapping starts at 100-200 K and increases rapidly below this temperature. For formaldehyde, it drops again at 20K. These two mechanisms present very different time scales. In Fig. 2, the probability of finished trajectories versus the propagation time are shown for several temperatures to illustrate the different time scales of the direct reaction and trapping mechanisms for the case of H<sub>2</sub>CO + OH reaction. For temperatures above 200 K, all trajectories finish before 0.1 ns. At 200 K, it can be observed that there is a second elbow for times longer than 1 ns, but it only accounts for less than 5 %. For formaldehyde at 100 K, this elbow seems to shift to even longer times and a large percentage of trajectories,  $\approx 20\%$ , remains trapped for times longer than 20 ns. Similar results are found for methanol at 200K. To make the calculations affordable, the maximum time has been reduced for temperatures where trapping dominates to make the calculations affordable. Many checks have been done at 100 K for the H<sub>2</sub>CO + OH reaction, where the trapping mechanism starts to be important, as explained in the SI.

All trapped trajectories were found in the well of the reactants, with geometries in between the two insets shown in Fig. 1. One typical RPMD trajectory for OH+ H<sub>2</sub>CO at 100K is shown in Fig. 3. The system starts an orbit, with relatively high end-over-end angular momentum. Along this orbit, the two systems are rotating initially and reoriented according to the long range dipole-dipole interaction. This first part of the trajectory, up to  $\approx 30$  ps, time at which the two reactants are at about 10 bohr, is the capture, which depends on the long range interaction. Dipole-dipole interaction is very effective in producing this capture, as already found with QCT calculations.<sup>17,24,25</sup>

Once the two reactants get closer, they start to rotate with respect to each other with a couple of rebounds in which the distance,  $R$ , between the two centers-of-mass increases. After some time, these large amplitude trajectories, similar to classical roaming trajectories,<sup>37–40</sup> stop and the two subsystems,  $\text{H}_2\text{CO}$  and  $\text{OH}$ , rotate around each other in a rather narrow interval of  $R$ , as if the excess of energy is dissipated in the beads. This second process of the trajectory can be associated to trapping, because a periodic-orbit-like motion starts and lasts longer than  $\approx 100$  ns. Along these orbits, the mutual orientation oscillates rapidly, in a pendular-like motion sampling a region close to the potential well.

A similar situation is also found for the second trajectory shown in Fig. 3 for  $\text{OH} + \text{H}_2\text{CO}$  at  $T = 20$  K. In this case, the number of high amplitude rebounds is lower, and the amplitude of the oscillations in  $\theta_{R-OH}$  ( $\mathbf{R}$  being the vector between the centers-of-mass of the two reactants) and  $\theta_{CO-OH}$  is reduced, but the end-over-end rotation, represented by  $\phi_R$  in the figure, is faster. This indicates that these long-lived complexes correspond to high rotational states, induced by reorientation of the two reactants along the orbit to approach each other, along the so-called capture process. This rotational excitation is “quantized” when using RPMD while in QCT calculations can be gradually switched on. This quantization introduces a constraint that at very low temperatures prevents the molecules from starting rotation at very long distances: in the RPMD case the available energy does not allow to increase an integer number the rotational quantum of the reactants needed to allow the reactants to reorient, reducing the capture probability. This explains why at 20 K, the trapping rate constant decreases, while in QCT calculation it continues growing.<sup>24</sup> The same roaming features are found for  $\text{OH} + \text{CH}_3\text{OH}$  reaction, showing a high rotational excitation with the relative position of the two reactants facing each other.

The fact that these trajectories are captured in the collision complex for such a long time is due to quantum effects. In the previous QCT study,<sup>17,24,25</sup> the lifetime of the collision complexes was analyzed, and never exceeded 50 ps, while in the present RPMD study this time is longer than 100 ns. According to the RRKM statistical theory,<sup>41,42</sup> the lifetime of the collision complex depends on the number of open channels,  $N_o(E)$ , as

$$\tau = 2\pi\hbar \frac{\rho(E)}{N_o(E)}, \quad (2)$$

where  $\rho(E)$  is the density of states of the complex at energy  $E$ . In the RPMD, where quantum ZPE and tunneling effects are included, the number of accesible states of the reactants,  $N_o(E)$ , is much lower than in the classical simulations, what explains why the RPMD collision lifetimes are much longer.

$\rho(E)$  is associated to the bound states of the collision complex in the potential well. If the separation of these bound states is lower than their width,  $\Gamma$ , associated to redissociation and tunneling, the statistical limit associated to large molecules is reached.<sup>43–47</sup> The initial state irreversibly decays in this dense manifold of bound states, and they rarely escape because of the low density of dissociation channels. This situation explains the results of the RPMD calculations. These bound states are rotationally excited, and only can redissociate

back to the reactants by rotational predissociation. Because the angular momentum conservation law introduces many constraints, it is very unlikely to stop the rotations of the two reactants to nearly zero angular momenta by transferring their energy back to the relative kinetic energy.

The extremely long collision complex lifetimes get closer to the tunneling timescale necessary to react. In this sense, this ZPL model is similar to the dimer19 and HPL-TST models,<sup>22,23</sup> without needing to reduce the energy of the complex below the redissociation threshold by collisions with third bodies. Since in this zero pressure model the energy is higher than in the HPL model, the tunneling is also faster.

The total reaction rate constant is given by

$$k(T) = k_{dir}(T) + k_{CF}(T), \quad (3)$$

where  $k_{dir}(T)$  is the direct reaction rate constant defined above and  $k_{CF}(T)$  is the complex forming reaction rate constant given by

$$k_{CF}(T) = k_{trap}(T) \frac{k_{tunnel}(T)}{k_{tunnel}(T) + k_{rediss}(T)}. \quad (4)$$

The challenge is to calculate the tunneling rate constant,  $k_{tunnel}(T)$ , and the redissociation rate,  $k_{rediss}(T)$ , under similar conditions, since they involve different processes and degrees of freedom.

In the  $\text{H}_2\text{CO}+\text{OH}$  reaction the barrier is quite low, and we can assume that anharmonic effects can reduce it sufficiently to justify the classical results. For this reason, we consider that the  $k_{tunnel}/[k_{tunnel} + k_{rediss}]$  ratio can be approximated by the reaction probability found in the QCT calculations of Refs.17,24. The QCT reaction probability is  $\approx 2\%$  for energies below 5 meV (see Fig. 10 of Ref.24). Using this value, the total reaction rate constant obtained with the RPMD method, Eq. (3), is calculated and presented in Fig. 4, and is compared with the previous QCT results<sup>17,24</sup> and the available experimental data.<sup>17,48,49</sup> The RPMD results are in a rather good agreement with the QCT results from 50 to 300 K, while the reduction obtained at 20 K with the RPMD method is not reproduced by the QCT results, as discussed above. The good agreement above 50 K is explained by the trapping mechanism, which involves essentially rotational degrees of freedom, whose quantification only plays a role at the lowest temperature of 20 K. Also, the barrier is sufficiently low so that it may be considered as submerged by the anharmonic effects. The comparison with experimental data is also reasonable in  $\text{H}_2\text{CO} + \text{OH}$ , showing a semiquantitative agreement above 50 K, and a good qualitative behavior. The difference between the experiments and these calculations above 200 K by a factor between 2-3 is attributed to the accuracy of the PES, and work is currently in progress to improve it.

The RPMD calculations performed for the CH<sub>3</sub>OH + OH reaction show very similar features to that of H<sub>2</sub>CO + OH, in particular the trapping below 200 K following the same roaming mechanism. The direct reaction rate constant between 300 and 500 K is in very good agreement with the low pressure limit (LPL-CCUS) results of Gao and co-workers,<sup>22</sup> and the transition to the trapping mechanism occurs at 200 K, where the two mechanisms coexist. Below 200 K, the direct mechanism is completely negligible, and the trapping mechanism dominates. As in the OH + H<sub>2</sub>CO case, the lifetime of the collision complex is longer than 50 ns at 50 K, and this lifetime should increase at lower temperatures.

The RPMD trapping rate constants in Table 1 increase very sharply from 200 to 50 K. For lower temperatures,  $k_{trap}$  is expected to stabilize or decrease as for the H<sub>2</sub>CO reaction. In this temperature regime, the RPMD  $k_{trap}(T)$  can be compared with the capture rate coefficients,  $k_a^{TST}(T)$ , calculated within a TST formalism by Ocaña et al.,<sup>23</sup> listed in their Table 4.  $k_a^{TST}(T)$  in Ref.23 varies from the minimum at 150 K of  $3.22 \cdot 10^{-11} \text{ cm}^3/\text{s}$  to  $4.31 \cdot 10^{-11} \text{ cm}^3/\text{s}$  at 30 K, while the RPMD trapping rate constants,  $2.98 \cdot 10^{-10} > k_{trap}(T) > 1.80 \cdot 10^{-10} \text{ cm}^3/\text{s}$ , is  $\approx 5$  times larger. The RPMD method is considered to be more accurate,<sup>31</sup> because it includes quantum effects (ZPE and tunneling), treats all degrees of freedom on an equal footing, and is based on real-time propagation of collision dynamics using the full PES, not only the stationary points.

The low pressure rate constant,  $k_{LPL}^{TST}(T)$ , calculated in Ref.23 must then be multiplied by the same factor of 5, leading to a considerably larger reaction rate constant, much closer to the measured one. This implies firstly that the pressure effects are less important and secondly, and more important for astrochemical models, that the zero pressure reaction rate constant also increases when lowering temperature. In order to calculate the complex forming rate constant,  $k_{CF}(T)$ , the ratio  $k_{tunnel}/[k_{tunnel} + k_{rediss}]$  has to be calculated. This branching ratio can be directly obtained from Ref.23 as  $k_{LPL}/k_a(T)$ , from their Eq.(E6). The branching ratio takes the values of 0.16, 0.045 and 0.016 at T=50, 100 and 200 K, respectively. Using these values the total reaction rate constant in the zero pressure limit is obtained using Eqs.(3) and (4), where  $k_{trap}(T)$  and  $k_{dir}(T)$  are directly calculated with the RPMD method, and  $k_{tunnel}/[k_{tunnel} + k_{rediss}] = k_{LPL}/k_a(T)$  is taken from the TST calculations of Ref.,<sup>23</sup> and it is compared with the experimental data in Fig. 5.

The agreement obtained with the experimental data for the CH<sub>3</sub>OH + OH reaction is really good, but further theoretical analysis should be done to completely confirm the results. In particular, the calculation of the  $k_{tunnel}/[k_{tunnel} + k_{rediss}]$  ratio as a function of temperature has to be recalculated including more dimensions.

In summary, we can conclude that reactions of formaldehyde and methanol with OH at the ZPL proceed via very long lived collision complexes and the reaction rate constant increases at low temperatures. The present RPMD study shows that it is of paramount importance to include ZPE and tunneling quantum effects giving rise to new dynamical features such as quantum roaming which play a major role in the reaction mechanisms. The complex mechanism at the zero pressure limit is an alternative that must coexist with the high pressure models already used,<sup>22,23</sup> with many aspects in common. Since in these studies

the relative weight of the LPL and HPL rate constants are fitted to the experimental results, it is of great interest to evaluate the LPL capture rate as accurately as possible. At this regard, the RPMD method used here is very accurate considering multidimensional quantum effects, and it is considered to yield better results than the TST approach beyond mono-dimensional model.

The behavior below 100 K, could also be explained by the pressure effects in the experiments, as suggested in previous TST studies.<sup>22,23</sup> In fact, the collision complexes live considerably longer than 100 ns, time of the order of magnitude of the collisions with the buffer gas. Under these conditions, it is therefore possible that the OM-OH complex collides with the BG, thus producing an energy change of the complex. If this energy increases, the reaction over the barrier is facilitated. If the energy decreases, the complex can only tunnel towards products, but at even longer time scales than the zero pressure mechanism presented here.

The extremely long lifetime of the collision complexes is then of high importance in interpreting the measurements. The reaction rate constants in CRESU experiments are obtained following the disappearance of the OH radical by laser induced fluorescence (LIF) technique. The loss of OH radicals can be due not only to the reaction with formaldehyde or methanol, but also by complexation. An experimental evidence of products or collision complexes at very low temperatures would be desirable indeed. For the OH + methanol reaction, the Leeds group detected CH<sub>3</sub>O radicals (one of the products) at 80 K, demonstrating that the reaction occurs at this low temperature.<sup>11</sup> However, quantification was not possible by LIF, which is necessary to determine the branching ratio of different products.

The CRESU experimental set up can follow the reaction dynamics in a limited time scale of around several hundreds of microseconds imposed by the uniformity length of the gas temperature and pressure. Therefore, if the trapped complexes, formed by either quantum LPL or HPL mechanisms, live longer, their fragmentation cannot be studied. In the present quantum LPL mechanism at 100K a lower limit of the complex lifetimes of > 200 or 50 ns are found in the two cases. For lower temperatures this complex lifetime is expected to increase significantly. The quantitative measurement of the products ratio would allow to address this point.

In astrophysical environments, the gas density is extremely low and high pressure conditions are not achieved. It is therefore of great importance to determine the individual rate constants of the quantum LPL for pressure-dependent reactions. This problem is a challenge for theory and experiment. For theory, the accurate determination of the full dimensional potential and the accuracy of RPMD or any other dynamical method to describe realistically the complex lifetimes are currently open questions. From the experimental side, the low gas densities of the interstellar medium are impossible to reach and the quantitative measurement of product branching ratios and the spectroscopic study of long-lived intermediates are now-a-days a challenge.



## Supplementary Material

Refer to Web version on PubMed Central for supplementary material.

## Acknowledgement

PdM, AA, EJ and OR acknowledge the support of the Ministerio de Economía y Competitividad (SPAIN) under grant No. FIS2017-83473-C2 and from the European Research Council under the European Union's Seventh Framework Programme (FP/2007-2013)/ERC Grant Agreement no. 610256 (NANOCOSMOS). YVS acknowledge the support of the European Regional Development Fund and the Republic of Cyprus through the Research Promotion Foundation (Project: INFRASTRUCTURE/1216/0070). The calculations have been performed at CESGA (finisterrae2), CENITS (lusitania2) and SCAYLE (calendula) supercomputer centers under RES (Red Española de Supercomputación) computational grant nos. AECT-2018-2-0001, AECT-2018-3-0001 and AECT-2019-1-0001.

## References

- (1). Atkinson R. Gas-phase tropospheric chemistry of organic compounds: a review. *Atmospheric Environment*. 1990; 24A:1.
- (2). Heard D, Pilling MJ. Measurement of OH and HO<sub>2</sub> in the troposphere. *Chem Rev*. 2003; 103:5163. [PubMed: 14664647]
- (3). Baulch DL, Cobos CJ, Cox RA, Esser C, Frank P, Just T, Kerr JA, Pilling MJ, Troe J, Walker RW, et al. Evaluated Kinetic Data for Combustion Modelling. *Journal of Physical and Chemical Reference Data*. 1992; 21:411–734.
- (4). Heard DE. Rapid Acceleration of Hydrogen Atom Abstraction Reactions of OH at Very Low Temperatures through Weakly Bound Complexes and Tunneling. *Accounts of Chemical Research*. 2018; 51:2620–2627. [PubMed: 30358991]
- (5). Tielens AGGM, Hagen W. Model calculations of the molecular composition of interstellar grain mantles. *Astron Astrophys*. 1982; 114:245.
- (6). Garrod R, Park IH, Caselli P, Herbst E. Are gas-phase models of interstellar chemistry tenable? The case of methanol. *Faraday Discuss*. 2006; 133:51. [PubMed: 17191442]
- (7). Watanabe N, Mouri O, Nagaoka A, Chigai T, Kouchi A, Pirronello V. Laboratory simulation of competition between hydrogenation and photolysis in the chemical evolution of H<sub>2</sub>O-CO ice mixtures. *AstroPhys J*. 2007; 668:1001.
- (8). Herbst E, van Dishoeck EF. Complex Organic Interstellar Molecules. *Annu Rev Astro Astrophys*. 2009; 47:427.
- (9). Cruz-Diaz GA, Martín-Doménech R, Muñoz-Caro GM, Chen Y-J. The negligible photodesorption of methanol ice and the active photon-induced desorption of its irradiation products. *Astron Astrophys*. 2016; 592:68.
- (10). Bertin M, Romanzin C, Doronin M, Philippe L, Jeseck P, Ligterink N, Linnartz H, Michaut X, Fillion J-H. UV photodesorption of methanol in pure and CO-rich ices: desorption rates of the intact molecule and of the photofragments. *AstroPhys J L*. 2016; 817:L12.
- (11). Shannon RJ, Blitz MA, Goddard A, Heard DE. Accelerated chemistry in the reaction between the hydroxyl radical and methanol at interstellar temperatures facilitated tunnelling. *Nature Chem*. 2013; 5:745. [PubMed: 23965675]
- (12). Gómez-Martín JC, Caravan RL, Blitz MA, Heard DE, Plane JMC. Low temperature kinetics of the CH<sub>3</sub>OH + OH reaction. *J Phys Chem A*. 2014; 118:2693. [PubMed: 24669816]
- (13). Caravan RL, Shannon RJ, Lewis T, Blitz MA, Heard DE. Measurements of Rate Coefficients for Reactions of OH with Ethanol and Propan-2-ol at Very Low Temperatures. *J Phys Chem A*. 2015; 119:7130. [PubMed: 25216323]
- (14). Antiñolo M, Agúndez M, Jiménez E, Ballesteros B, Canosa A, Dib GE, Albadalejo J, Cernicharo J. Reactivity of OH and CH<sub>3</sub>OH between 22 and 64 K: modeling the gas phase production of CH<sub>3</sub>O in Barnard 1b. *AstroPhys J*. 2016; 823:25. [PubMed: 27279655]

- (15). Shannon RJ, Taylor S, Goddard A, Blitz MA, Heard DE. Observation of a large negative temperature dependence for rate coefficients of reactions of OH with oxygenated volatile organic compounds studied at 86-112 K. *Phys Chem Chem Phys.* 2010; 12:13511. [PubMed: 20859585]
- (16). Jimenez E, Antiñolo M, Ballesteros B, Canosa A, Albaladejo J. First evidence of the dramatic enhancement of the reactivity of methyl formate (HC(O)OCH<sub>3</sub>) with OH at temperatures of the interstellar medium: a gas-phase kinetic study between 22 K and 64 K. *Phys Chem Chem Phys.* 2016; 18:2183. [PubMed: 26691336]
- (17). Ocaña AJ, Jiménez E, Ballesteros B, Canosa A, Antiñolo M, Albaladejo J, Agúndez M, Cernicharo J, Zanchet A, del Mazo P, et al. Is the gas phase OH+H<sub>2</sub>CO reaction a source of HCO in interstellar cold dark clouds? A kinetic, dynamics and modelling study. *AstroPhys J.* 2017; 850:28. [PubMed: 29880977]
- (18). Ocaña AJ, Blázquez S, Ballesteros B, Canosa A, Antiñolo M, Albaladejo J, Jimenez E. Gas phase kinetics of the OH + CH<sub>3</sub>CH<sub>2</sub>OH reaction at temperatures of the interstellar medium (T = 21-107 K). *Phys Chem Chem Phys.* 2018; 20:5865. [PubMed: 29417104]
- (19). Siebrand W, Smedarchina Z, Martínez-Núñez E, Fernández-Ramos A. Methanol dimer formation drastically enhances hydrogen abstraction from methanol by OH at low temperature. *Phys Chem Chem Phys.* 2016; 18:22712. [PubMed: 27479134]
- (20). Shannon RJ, Gomez Martin JC, Caravan RL, Blitz MA, Plane JMC, Heard DE, Antiñolo M, Agundez M, Jimenez E, Ballesteros B, et al. Comment on "Methanol dimer formation drastically enhances hydrogen abstraction from methanol by OH at low temperature" by W. Siebrand, Z. Smedarchina, E. Martinez-Nunez and A. Fernandez-Ramos, *Phys. Chem. Chem. Phys.*, 2016, 18, 22712. *Phys Chem Chem Phys.* 2018; 20:8349. [PubMed: 29492495]
- (21). Siebrand W, Smedarchina Z, Ferro-Costas D, Martínez-Núñez E, Fernández-Ramos A. Reply to the Comment on "Methanol dimer formation drastically enhances hydrogen abstraction from methanol by OH at low temperature" by D. Heard, R. Shannon, J. Gomez Martin, R. Caravan, M. Blitz, J. Plane, M. Antiñolo, M. Agundez, E. Jimenez, B. Ballesteros, A. Canosa, G. El Dib, J. Albaladejo and J. Cernicharo, *Phys. Chem. Chem. Phys.*, 2018, 20, 8349. *Phys Chem Chem Phys.* 2018; 20:8355. [PubMed: 29498727]
- (22). Gao LG, Zheng J, Fernández-Ramos A, Truhlar DG, Xu X. Kinetics of the Methanol Reaction with OH at Interstellar, Atmospheric, and Combustion Temperatures. *Journal of the American Chemical Society.* 2018; 140:2906–2918. [PubMed: 29299932]
- (23). Ocaña AJ, Blázquez S, Potapov A, Ballesteros B, Canosa A, Antiñolo M, Vereecken L, Albaladejo J, Jiménez E. Gas-phase reactivity of CH<sub>3</sub>OH toward OH at interstellar temperatures (11.7-177.5 K): Experimental and theoretical study. *PCCP.* 2019; doi: 10.1039/C9CP00439D
- (24). Zanchet A, del Mazo P, Aguado A, Roncero O, Jiménez E, Canosa A, Agúndez M, Cernicharo J. Full dimensional potential energy surface and low temperature dynamics of the H<sub>2</sub>CO + OH → HCO + H<sub>2</sub>O reaction. *PCCP.* 2018; 20:5415. [PubMed: 28959812]
- (25). Roncero O, Zanchet A, Aguado A. Low temperature reaction dynamics for CH<sub>3</sub>OH + OH collisions on a new full dimensional potential energy surface. *Phys Chem Chem Phys.* 2018; 20:25951. [PubMed: 30294740]
- (26). Guo H. Quantum dynamics of complex-forming bimolecular reactions. *Int Rev Phys Chem.* 2012; 31:1.
- (27). Craig IR, Manolopoulos DE. Quantum statistics and classical mechanics: Real time correlation functions from ring polymer molecular dynamics. *J Chem Phys.* 2004; 121:3368. [PubMed: 15303899]
- (28). Craig IR, Manolopoulos DE. Chemical reaction rates from ring polymer molecular dynamics. *J Chem Phys.* 2005; 122:084106.
- (29). Craig IR, Manolopoulos DE. A refined ring polymer molecular dynamics theory of chemical reaction rates. *J Chem Phys.* 2005; 123:034102.
- (30). Suleimanov YV, Collepardo-Guevara R, Manolopoulos DE. Bimolecular reaction rates from ring polymer molecular dynamics: application to H + CH<sub>4</sub> → H<sub>2</sub> + CH<sub>3</sub>. *J Chem Phys.* 2011; 134:044131. [PubMed: 21280711]

- (31). Suleimanov YV, Aoiz FJ, Guo H. Chemical reaction rate coefficients from Ring polymer molecular dynamics: theory and practical applications. *J Phys Chem A*. 2016; 120:8488. [PubMed: 27627634]
- (32). Pérez de Tudela R, Aoiz FJ, Suleimanov YV, Manolopoulos DE. Chemical Reaction Rates from Ring Polymer Molecular Dynamics: Zero Point Energy Conservation in  $\text{Mu} + \text{H}_2 \rightarrow \text{MuH} + \text{H}$ . *The Journal of Physical Chemistry Letters*. 2012; 3:493–497. [PubMed: 26286053]
- (33). Pérez de Tudela R, Suleimanov YV, Richardson JO, Sáez Rábanos V, Green WH, Aoiz FJ. Stress Test for Quantum Dynamics Approximations: Deep Tunneling in the Muonium Exchange Reaction  $\text{D} + \text{HMu} \rightarrow \text{DMu} + \text{H}$ . *The Journal of Physical Chemistry Letters*. 2014; 5:4219–4224. [PubMed: 26278957]
- (34). Suleimanov YV, Aguado A, Gómez-Carrasco S, Roncero O. Ring Polymer Molecular dynamics approach to study the transition between statistical and direct mechanisms in the  $\text{H}_2 + \text{H}_3^+ \rightarrow \text{H}_3^+ + \text{H}_2$  reaction. *J Phys Chem Lett*. 2018; 9:2133. [PubMed: 29633841]
- (35). Suleimanov Y, Allen J, Green W. RPMDrate: Bimolecular chemical reaction rates from ring polymer molecular dynamics. *Computer Physics Communications*. 2013; 184:833–840.
- (36). Andersen HC. Molecular dynamics simulations at constant pressure and/or temperature. *The Journal of Chemical Physics*. 1980; 72:2384–2393.
- (37). Townsend D, Lahankar SA, Lee SK, Chamreau S, Suits AG, Zhang X, Rheinecker J, Harding LB, Bowman JM. The Roaming Atom: Straying from the Reaction Path in Formaldehyde Decomposition. *Science*. 2004; 306:1158. [PubMed: 15498970]
- (38). Harding LB, Georgievskii Y, Klippenstein SJ. Roaming radical kinetics in the decomposition of Acetaldehyde. *J Phys Chem A*. 2010; 114:765. [PubMed: 20038152]
- (39). Ulusoy IS, Stanton JF, Hernandez R. Effects of roaming trajectories on the transition state theory rates of a reduced-dimensional model of ketene isomerization. *J Phys Chem A*. 2013; 117:10567.
- (40). Bowman JM, Houston PL. Theories and simulations of roaming. *Chem Soc Rev*. 2017; 46:7615. [PubMed: 28979955]
- (41). Marcus RA. *J Chem Phys*. 1952; 20:352.
- (42). Marcus RA. *J Chem Phys*. 1952; 20:355.
- (43). Bixon M, Jortner J. Long radiative lifetimes of small molecules. *J Chem Phys*. 1969; 50:3284.
- (44). Freed K, Nitzan A. Intramolecular vibrational energy redistribution and the time evolution of molecular fluorescence. *J Chem Phys*. 1980; 73:4765.
- (45). Uzer T. Theories of intramolecular vibrational energy transfer. *Phys Reports*. 1991; 199:73.
- (46). Miller W. Appendix on Theories of intramolecular vibrational energy transfer. *Phys Reports*. 1991; 199:73.
- (47). Roncero O, Caloto D, Janda KC, Halberstadt N. From the Sparse to the Statistical Limit of Intramolecular Vibrational Redistribution in Vibrational Predissociation:  $\text{ArCl}_2$  as an example. *J Chem Phys*. 1997; 107:1406.
- (48). Sivakumaran V, Hölscher D, Dillon T, Crowley JN. Reaction between OH and HCHO: temperature dependent rate coefficients (202–399 K) and product pathways (298 K). *Phys Chem Chem Phys*. 2003; 5:4821.
- (49). Wang S, Davidson DF, Hanson RK. High temperature measurements for the rate constants of  $\text{C}_1$ - $\text{C}_4$  aldehydes with OH in a shock tube. *Proc Combust Inst*. 2015; 35:473.

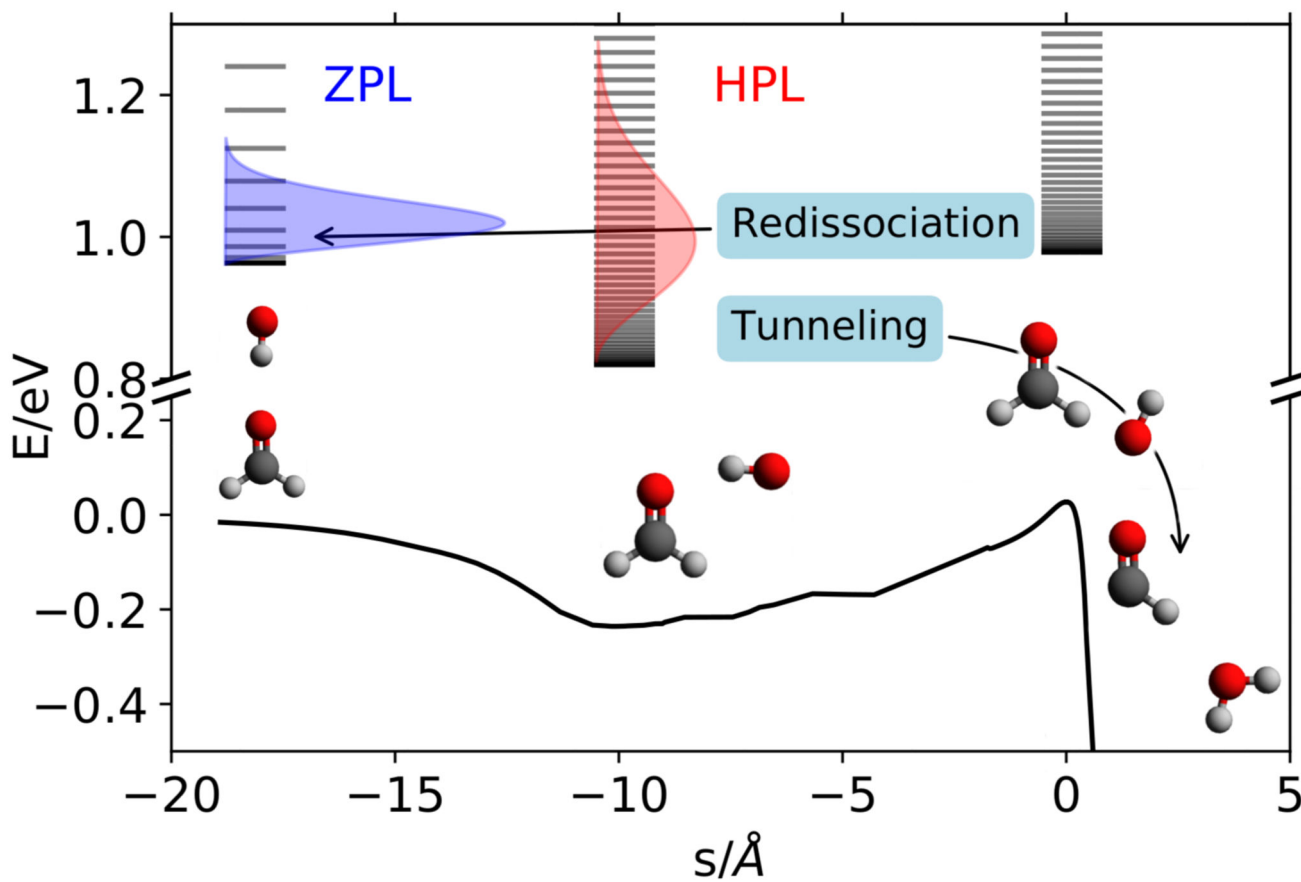


**Figure 1.**  
Energy diagram of the  $\text{H}_2\text{CO} + \text{OH} \rightarrow \text{HCO} + \text{H}_2\text{O}$  reaction.

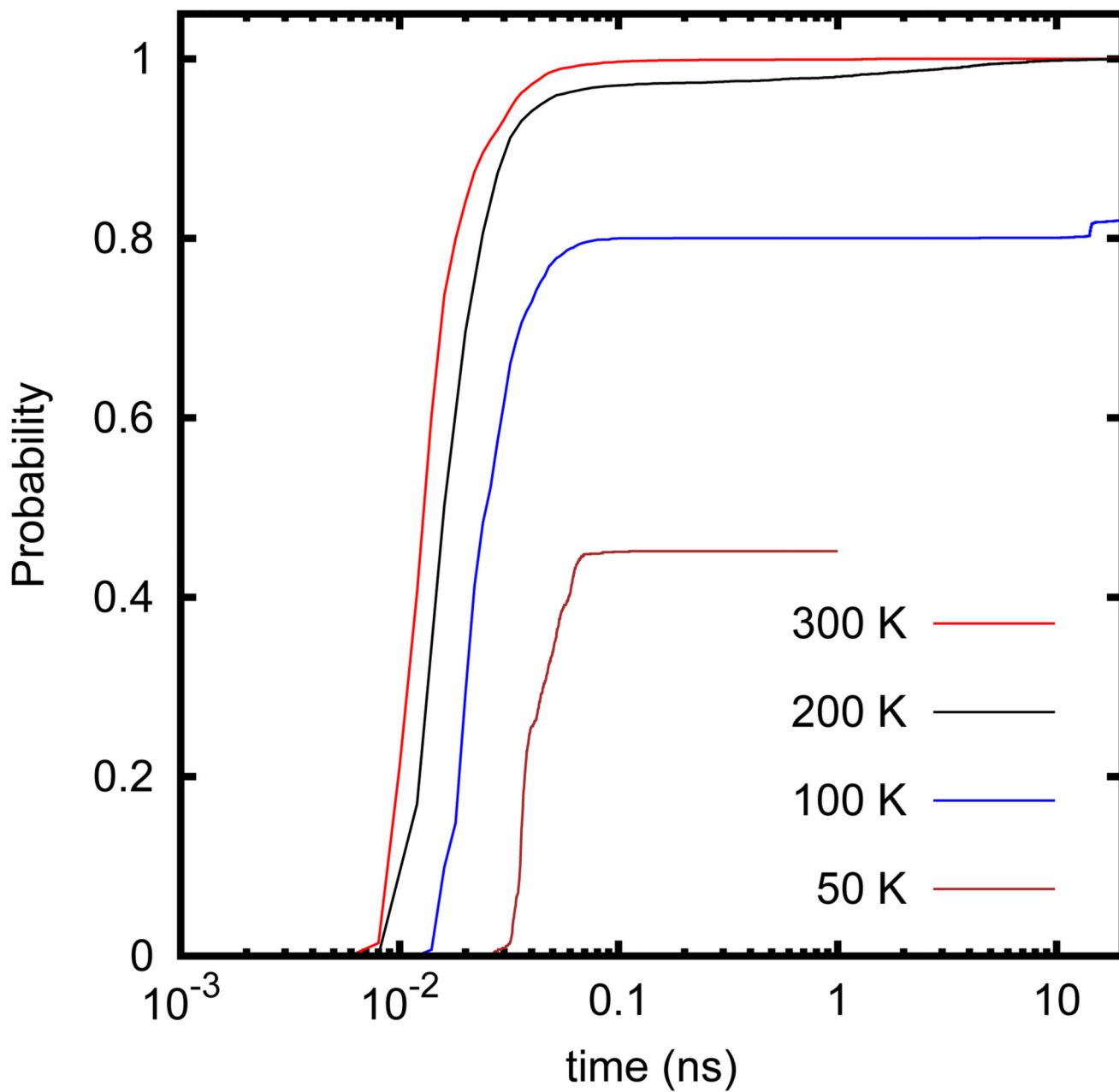


**Figure 2.**  
Finished trajectories versus propagation time for the  $\text{H}_2\text{CO} + \text{OH}$  reaction.

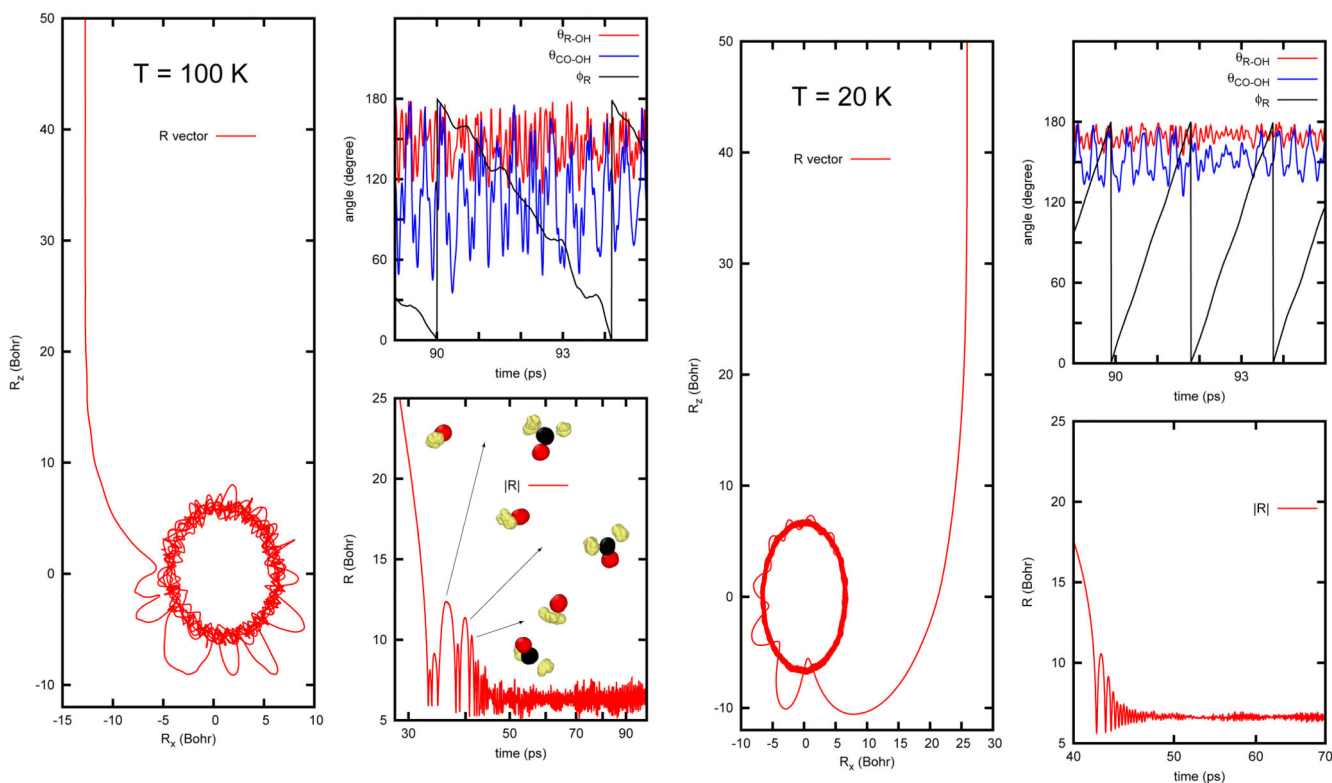


**Figure 3.**

Evolution of the vector  $\mathbf{R}$ , between the centers-of-mass of reactants using the centroid for a RPMD trajectory at 100 K with initial impact parameter  $b^{\text{trap}}=13$  bohr (left panels), and at 20 K with  $b^{\text{trap}}=26$  bohr (right panels). In the upper right panels, the evolution of the angles between  $\mathbf{R}$  and  $\mathbf{r}_{\text{OH}}$  and  $\mathbf{r}_{\text{CO}}$  and  $\mathbf{r}_{\text{OH}}$  are displayed for a short period of time. The angle  $\phi_{\text{R}} = \arctan(R_x/R_z)$  represents the end-over-end rotation of OH with respect to  $\text{H}_2\text{CO}$ . Similar roaming patterns are found for the OH + methanol case.

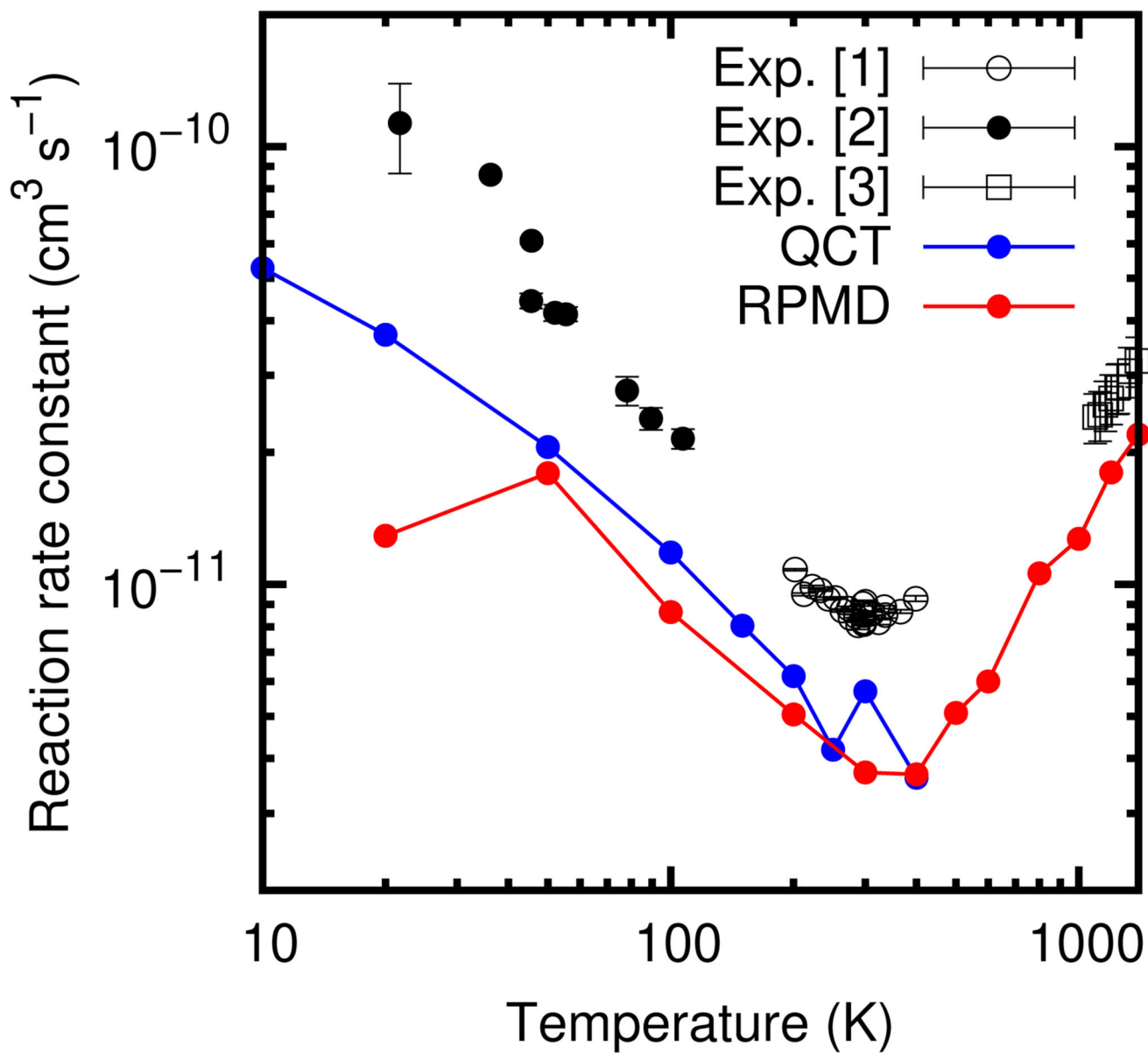


**Figure 4.** RPMD rate constants for the  $\text{H}_2\text{CO} + \text{OH} \rightarrow \text{HCO} + \text{H}_2\text{O}$  reaction, obtained using Eq. (3). The QCT results are taken from Ref.17,24 Exp[1] are from Ref.48 Exp[2] are from Ref.17 Exp[3] are from Ref.49

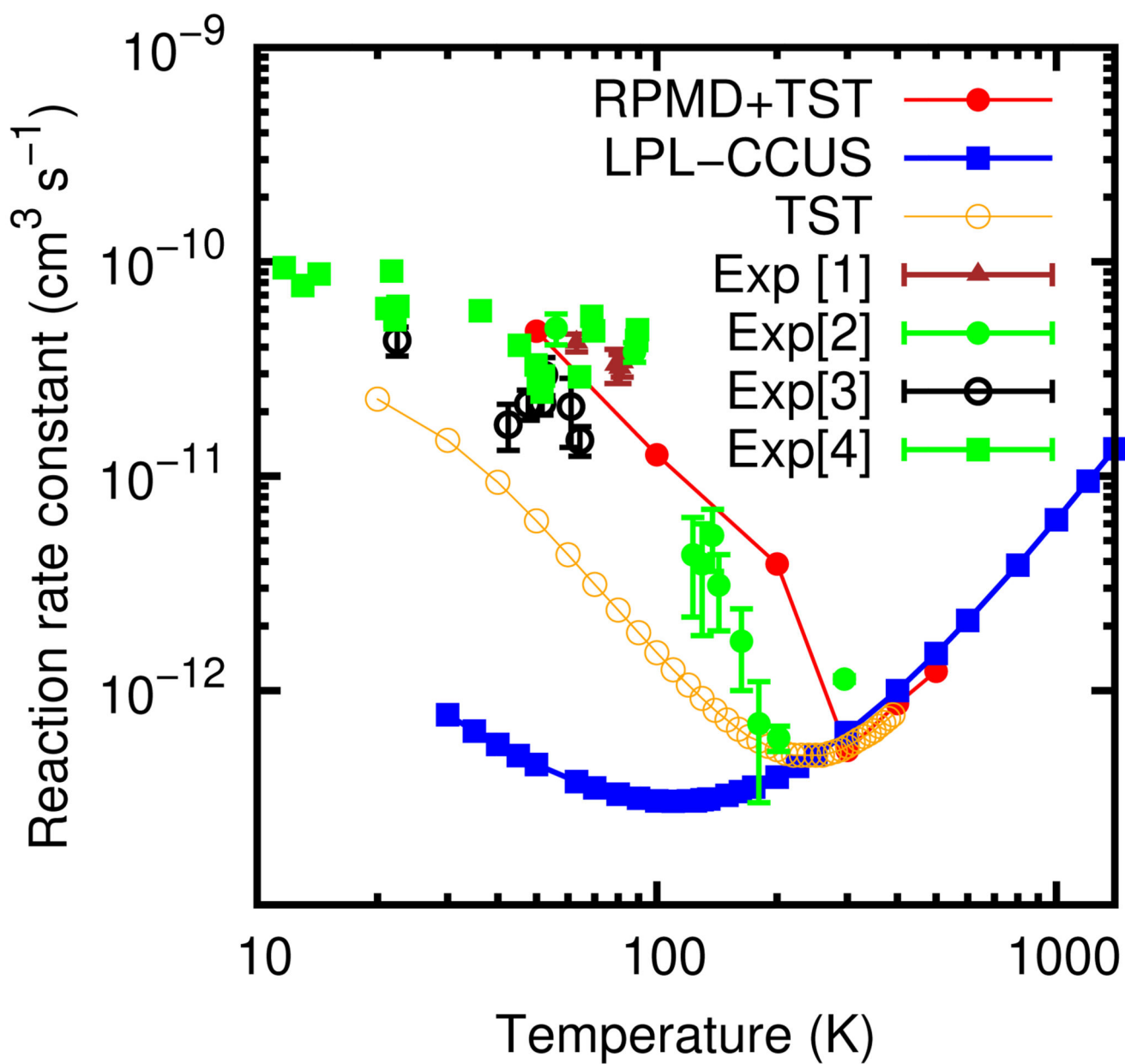


**Figure 5.** Total reaction rate constant for CH<sub>3</sub>OH+OH reaction at the zero pressure limit calculated using Eq. (??) combining RPMD and TST results as explained in the text. The [1,2,3,4] experimental results are from Refs.,11,12,14,23 respectively. LPL-CCUS are taking from Ref.22 TST refers to the TST (RRKM) results obtained in the LPL in Ref.23



**Table 1**  
Parameters of the direct RPMD trajectory calculations, and calculated rate constants.

T(K)	$N_{beads}$	$N_{tot}$	$t_{max}$ (ns)	$b_{max}^{react}$ (bohr)	$b_{max}^{trab}$ (bohr)	$P_{dir}$	$P_{trap}$	$k_{dir}$ ( $\text{cm}^3/\text{s}$ )	$k_{trap}$ ( $\text{cm}^3/\text{s}$ )
<b>H<sub>2</sub>CO + OH</b>									
1400	48	10000	20	8.08	0	0.043	0.0	$2.20 \cdot 10^{-11}$	0.0
1200	48	10000	20	7.27	0	0.047	0.0	$1.80 \cdot 10^{-11}$	0.0
1000	64	12000	20	7.49	0	0.033	0.0	$1.27 \cdot 10^{-11}$	0.0
800	64	10000	20	7.60	0	0.030	0.0	$1.06 \cdot 10^{-11}$	0.0
600	64	10000	20	10.78	0	0.009	0.0	$6.00 \cdot 10^{-12}$	0.0
500	96	10000	20	10.43	0	0.009	0.0	$5.09 \cdot 10^{-12}$	0.0
400	96	10000	20	10.05	0	0.008	0.0	$3.68 \cdot 10^{-12}$	0.0
300	128	10000	20	10.59	0	0.007	0.0	$3.72 \cdot 10^{-12}$	0.0
200	256	10000	20	13.15	0	0.007	0.0	$5.05 \cdot 10^{-12}$	0.0
100	384	5000	20	13.40	16.00	0.008	0.20	$5.10 \cdot 10^{-12}$	$1.77 \cdot 10^{-10}$
50	768	3000	1	8.63	22.07	0.017	0.55	$3.51 \cdot 10^{-12}$	$7.22 \cdot 10^{-10}$
20	1920	3000	1	12.30	26.85	0.003	0.48	$8.90 \cdot 10^{-13}$	$6.01 \cdot 10^{-10}$
<b>CH<sub>3</sub>OH + OH</b>									
500	96	20000	50	8.95	0	0.003	0.0	$1.22 \cdot 10^{-12}$	0.0
400	96	20000	50	8.00	0	0.003	0.0	$8.70 \cdot 10^{-13}$	0.0
300	128	20000	50	8.52	0	0.002	0.0	$5.26 \cdot 10^{-13}$	0.0
200	192	10000	5	5.66	11.91	0.008	0.32	$1.01 \cdot 10^{-12}$	$1.80 \cdot 10^{-10}$
100	384	2000	5	0.0	13.44	0.0	0.46	0.0	$2.80 \cdot 10^{-10}$
50	768	2000	5	0.0	17.54	0.0	0.37	0.0	$3.06 \cdot 10^{-10}$